arXiv:gr-qc/0005012v1 3 May 2000

A Nearly Minimum Redundant Correlator Interpolation Formula for Gravitational Wave Chirp Detection

R.P. Croce, Th. Demma
Wavesgroup, D.I.^{3}E., Univ. of Salerno, Italy

V. Pierro, I.M. Pinto, F. Postiglione
Wavesgroup, Univ. of Sannio at Benevento, Italy

(December 2, 2024)

An absolute lower bound on the number of templates needed to keep the fitting factor above a prescribed minimal value Γ in correlator-bank detection of (newtonian) gravitational wave chirps from unknown inspiraling compact binary stars is derived, resorting to the theory of quasi band-limited functions in the L^∞ norm. An explicit nearly-minimum redundant cardinal-interpolation formula for the (reduced, noncoherent) correlator is introduced. Its computational burden and statistical properties are compared to those of the plain lattice of (reduced, noncoherent) correlators, for the same Γ. Extension to post-newtonian models is outlined.

PACS number(s): 04.80.Nn, 95.55.Ym, 95.75.Pq,97.80.Af

INTRODUCTION

The detection of gravitational wave (henceforth GW) chirps from unknown inspiraling compact binary sources (henceforth CBS) is a primary goal for the early operation of broadband interferometric detectors, including TAMA300 [1], GEO600 [2], the two LIGOs [3] and VIRGO [4], in view of the sizeable expected rate of observable events [5].

For additive gaussian stationary noise, the correlator-bank threshold-detector is the optimal one, yielding the smallest false-dismissal probability, at any fixed false-alarm probability and signal to noise ratio [6].

The issues of optimum template parametrization and placement, and the related computational burden have been discussed by several Authors [7]- [13]. A lucid account of the main relevant landmarks is given in [14].

Curiously, the question of possible *efficient* interpolation among the correlators has been left yet unsolved [14].

In this paper we set up and test an efficient interpolated representation of the (reduced, noncoherent) correlator for the simplest paradigm case of Newtonian chirps. The proposed representation [15] is proven to get close to the *absolute minimum* template density required by a prescribed minimal-match condition, which follows from the theory of quasi-bandlimited (henceforth q-BL) functions in the L^∞ norm. The statistical performance of the proposed representation are shown to be essentially equivalent to those of the plain lattice.

This paper is accordingly organized as follows. In Section I we recall a number of relevant concepts and results. In Section II we review the design of the plain template-bank for the simplest (Newtonian) case, and discuss its statistical detection properties. In Section III we briefly introduce q-BL functions and cardinal expansions, and derive the proposed expansions. In Section IV we compare the computational burden and the statistical detection/estimation properties of the cardinal-interpolated (reduced, noncoherent) correlator lattice to those of the plain lattice. Conclusions follow under Section V.

I. BACKGROUND

In this section we resume a number of well known concepts relevant to CBS chirp detection, and introduce the notation.

A. Noncoherent Correlator. Deflection and SNR

Detecting GW chirps from unknown inspiraling CBS requires the computation of a suitable set of non-coherent correlators (henceforth NCC) [16]:

$$c[\bar{T}] = 2\left|\int_{f_{inf}}^{f_{sup}} \frac{A(f)\bar{T}^*(f)}{\Pi(f)}\, df\right|, \tag{1.1}$$

where (f_{inf}, f_{sup}) is the useful antenna spectral window, $A(f)=S(f)+N(f)$ are the noise corrupted (spectral) data, resulting from the superposition of a (possibly null) signal $S(f)$ and a realization $N(f)$ of the antenna noise (assumed gaussian and stationary), $\bar{T}(f)$ is an element of a suitable set of unit-norm chirp-*templates* such that

$$||\bar{T}|| = \left|2\int_{f_{inf}}^{f_{sup}} \frac{\bar{T}(f)\bar{T}^*(f)}{\Pi(f)}\, df\right|^{1/2} = 1, \tag{1.2}$$

and $\Pi(f)$ is the (one-sided) antenna noise power spectral density (henceforth PSD). The random variables c have Ricean probability densities [6],

$$w(c) = c\exp\left(-\frac{c^2+d^2}{2}\right) I_0\left(c\,d\right), \tag{1.3}$$

where $I_0(\cdot)$ is the modified Bessel function of first kind and zero order, and

$$d = \left|2\int_{f_{inf}}^{f_{sup}} \frac{S(f)\bar{T}^*(f)}{\Pi(f)}\, df\right| \tag{1.4}$$

is the *deflection* obtained using $\bar{T}$. The moments of (1.3) can be written in terms of Kummer's confluent hypergeometric function [25]:

$$\langle c^n\rangle = 2^{n/2}\,\Gamma\left(1+\frac{n}{2}\right)\;{}_1F_1\left(-\frac{n}{2};1;-\frac{d^2}{2}\right). \tag{1.5}$$

For $d \gtrsim 5$ the riceans (1.3) merge into gaussians, with:

$$E\left[c\right] \approx d, \quad \mathrm{var}\left[c\right] \approx 1. \tag{1.6}$$

The deflection attains its maximum value iff the template $\bar{T}$ is *matched* to the signal, viz.:

$$\bar{T}(f) = \frac{S(f)}{||S(f)||}, \tag{1.7}$$

yielding:

$$d = d_{max} = \left|2\int_{f_{inf}}^{f_{sup}} \frac{S(f)S^*(f)}{\Pi(f)}\, df\right|^{1/2} =: SNR, \tag{1.8}$$

where SNR is the *intrinsic* signal-to-noise ratio.

B. Chirp Templates

The stationary phase principle (see [17] for a thorough discussion of its validity) can be used to show that the asymptotic principal part [18] of a general [19], [20], reduced [21] post newtonian (henceforth PN) chirp can be written [11]:

$$S(f;\phi_c,T_c,\vec{\xi}) = Af^{-7/6}\exp\left\{j\left[2\pi f T_c - \phi_c + \psi(f,\vec{\xi})\right]\right\}, \tag{1.9}$$

where A is a constant (real, unknown) amplitude factor, T_c is the (fiducial) coalescency time [22], ϕ_c is the template phase at $t=T_c$, and $\vec{\xi}$ represents the remaining *intrinsic* source parameters [26].
Equation (1.9) is used to construct the needed chirp templates. A further suffix T will be used to label the template parameters A_T, ϕ_{c_T}, T_{c_T}, and $\vec{\xi}_T$.
All template amplitudes A_T will be chosen so as to comply with the normalization condition (1.2), viz.:

$$A_T = \left[2\int_{f_{inf}}^{f_{sup}} \frac{f^{-7/3}}{\Pi(f)} df\right]^{-1/2}. \tag{1.10}$$

C. Maximum Likelihood Criterion. Fitting Factor

Equations (1.6) imply that (under the assumption of a uniform distribution of the unknown source parameters) the *largest* correlator will *most likely* correspond to the special template yielding the largest deflection (maximum likelihood (ML) estimation criterion [6]).
Data analysis for detecting chirps reduces thus to the following. Given the (spectral) noisy data, and a set (lattice) of templates, suitably covering the chirp parameter space, the corresponding (noncoherent) correlators $\{c_k | k = 1, 2, \ldots, N\}$ are computed. The *largest* among these correlators is used as a *detection statistic* [6], viz., whenever this latter exceeds a suitable threshold, set by the prescribed false-alarm probability (*surveillance* strategy [6]), a signal is declared to have been observed [24], and the corresponding template is taken as the *most likely* estimate of the observed signal [6].
It is convenient to measure the *goodness of fit* between a given signal $S(f)$ and the *best available* template in the set in terms of the so called *fitting factor* [27]:

$$FF = \max_k \frac{d_k}{SNR}. \tag{1.11}$$

The set of templates should be constructed in such a way that for *any* admissible signal,

$$FF \geq \Gamma, \tag{1.12}$$

where $1-\Gamma^3$ gauges the fraction of potentially observable sources which *could* be *lost* as an effect of template mismatch [28], [29].

D. The Reduced Correlator

In view of eq. (1.9), the noncoherent correlator (1.1) can be written:

$$c = \frac{\left| 2 \int_{f_{inf}}^{f_{sup}} \frac{A(f) f^{-7/6} e^{-j\psi_T(f,\vec{\xi})]}}{\Pi(f)} \exp(-j2\pi f T_{c_T}) df \right|}{\left[2 \int_{f_{inf}}^{f_{sup}} \frac{f^{-7/3}}{\Pi(f)} df \right]^{1/2}}. \tag{1.13}$$

Equation (1.13) is formally (but for inessential factors) the absolute value of the $(f \to T_{c_T})$ Fourier transform of the (complex-valued) function:

$$K(f) = \begin{cases} \dfrac{A(f)\bar{T}^*(f;0,0,\vec{\xi})}{\Pi(f)}, & f_{inf} \leq f \leq f_{sup} \\ 0, & f < f_{inf},\ f > f_{sup}. \end{cases} \tag{1.14}$$

Maximizing the noncoherent correlator (1.13) w.r.t. T_{c_T}, is thus equivalent to taking the *largest* absolute value of the $(f \to T_{c_T})$ Fourier transform of (1.14). The resulting *reduced* correlator [30] will be denoted with a capital letter, viz.:

$$C = \sup_{T_{c_T}} c\ . \tag{1.15}$$

E. The Newtonian Deflection and the Match

For illustrative purposes, in this paper we shall restrict to the simplest Newtonian ($0PN$) signals and templates. The $0PN$ function $\psi_T(f;\vec{\xi})$ in (1.9) reads:

$$\psi_T(f) = \frac{3}{128} \left(\frac{\pi G}{c^3} \right)^{-5/3} \mathcal{M}_T^{-5/3} f^{-5/3}, \tag{1.16}$$

where $\mathcal{M}_T$ is the template chirp-mass. It is convenient to introduce the following dimensionless variables and parameters:

$$\bar{f} = \frac{f}{f_{inf}}, \quad \Theta = f_{inf}(T_c - T_{c_T}), \quad \bar{\mathcal{M}} = \frac{\mathcal{M}}{M_\odot},$$

$$\Delta = \bar{\mathcal{M}}_s^{-5/3} - \bar{\mathcal{M}}_T^{-5/3}, \quad \Lambda = \frac{3}{128}\left(\frac{\pi G f_{inf} M_\odot}{c^3}\right)^{-5/3}, \tag{1.17}$$

where $M_\odot$ is the solar mass, so as to recast the deflection (1.4) into the form:

$$d(\Delta,\Theta) = SNR \cdot \frac{\left|\int_1^{\bar{f}_{sup}} d\bar{f}\ \frac{\bar{f}^{-7/3}}{\Pi(\bar{f})} \exp\left[j(2\pi\Theta\bar{f} + \Lambda\bar{f}^{-5/3}\Delta\right]\right|}{\int_1^{\bar{f}_{sup}} d\bar{f}\ \frac{\bar{f}^{-7/3}}{\Pi(\bar{f})}}. \tag{1.18}$$

We also introduce the *reduced* deflection:

$$D(\Delta) = \max_\Theta d(\Delta,\Theta), \tag{1.19}$$

and the related normalized [31] functions:

$$\bar{d}(\cdot) = \frac{d(\cdot)}{SNR}, \quad \bar{D}(\cdot) = \frac{D(\cdot)}{SNR}. \tag{1.20}$$

The function $\bar{D}(\Delta)$ is known as the (newtonian) *match*. The quantity Γ in (1.12) is accordingly also named the *minimal match* [14].
The functions $\bar{d}$ and $\bar{D}$ are displayed in Fig.s 1 and 2, respectively, for the special case of a LIGO-like noise PSD,

$$\Pi(f) = \frac{\Pi_0}{5}\left\{\left(\frac{f_0}{f}\right)^4 + 2\left[1 + \left(\frac{f}{f_0}\right)^2\right]\right\}, \tag{1.21}$$

with $f_0 = 300Hz$ (Π_0 is a constant of no concern to us here), and for a spectral window with:

$$f_{inf} = 40Hz, \quad f_{sup} = 400Hz. \tag{1.22}$$

The value Θ_{max} of Θ which maximizes $\bar{d}(\Delta,\Theta)$ in a neighbourhood of $\Delta = 0$ is shown in Fig. 3 as a function of Δ.

II. THE PLAIN (NEWTONIAN) LATTICE

Given a range $[\mathcal{M}_{min}, \mathcal{M}_{max}]$ of allowed source chirp masses, let the set of template chirp-masses be:

$$\bar{\mathcal{M}}_1^{-5/3} = \bar{\mathcal{M}}_{max}^{-5/3}, \quad \bar{\mathcal{M}}_{n+1}^{-5/3} = \bar{\mathcal{M}}_n^{-5/3} + \delta_L, \quad n = 1, 2, \ldots, N_L - 1, \tag{2.1}$$

where δ_L is the lattice-spacing, and

$$N_L = \left\lceil \frac{\bar{\mathcal{M}}_{min}^{-5/3} - \bar{\mathcal{M}}_{max}^{-5/3}}{\delta_L} \right\rceil \tag{2.2}$$

is the total number of templates. Obviously Δ can take only the discrete values:

$$\Delta_n = \bar{\mathcal{M}}_s^{-5/3} - \bar{\mathcal{M}}_n^{-5/3}, \quad n = 1, 2, \ldots, N_L. \tag{2.3}$$

A. Lattice Design

Given $\bar{\mathcal{M}}_s$, the fitting factor of the lattice is:

$$FF = \max_n \bar{D}(\Delta_n) = \bar{D}\left(\min_n |\Delta_n|\right). \tag{2.4}$$

The minimal-match condition (1.12) should be obviously enforced in the worst case, where:

$$\bar{\mathcal{M}}_s^{-5/3} = \bar{\mathcal{M}}_q^{-5/3} + \frac{\delta_L}{2}, \tag{2.5}$$

yielding:

$$\bar{D}\left(\frac{\delta_L}{2}\right) = \Gamma. \tag{2.6}$$

Equation (2.6) uniquely determines the lattice spacing δ_L, and hence via (2.2) also the total number of templates.

B. False Alarm and False Dismissal Probabilities

The statistical distribution of the detection statistic

$$\max_k C_k = \max_h c_h \tag{2.7}$$

is *not* known in exact form, and one should resort to numerical simulations aided by intuition to compute the lattice false-alarm and false-dismissal probabilities.

The detection threshold γ is determined from the prescribed (tolerated) false alarm probability α, by solving the equation:

$$\alpha = \text{prob}[\exists\ k : C_k > \gamma | SNR = 0] = 1 - \text{prob}[\forall\ h, c_h < \gamma | SNR = 0]. \tag{2.8}$$

The joint probability in (2.8) is difficult to compute, since the c_h are *not* statistically independent in general. For most practical purposes, a decent approximation is:

$$\text{prob}[\forall\ h, c_h < \gamma | SNR = 0] = (1 - e^{-\gamma^2/2})^M, \tag{2.9}$$

which would be appropriate if the c_h were a collection of M *independent* ricean random variables. Numerical experiments suggest an almost linear dependence of M on the total number of NCC used [32].

The probability of *false dismissal* of a signal with $SNR \neq 0$ is:

$$\beta(\gamma, SNR) = \text{prob}[\max_k C_k < \gamma | SNR \neq 0] = \text{prob}[\forall h, c_h < \gamma | SNR \neq 0]. \tag{2.10}$$

A simple (conservative) approximation of (2.10) is [12], [33]:

$$\beta(\gamma, SNR) \approx \text{prob}[C_- < \gamma, C_+ < \gamma | SNR \neq 0], \tag{2.11}$$

where C_-, C_+ denote the reduced correlators corresponding to the nearest-neighbouring templates, with chirp masses $\bar{\mathcal{M}}_\pm$ such that $\bar{\mathcal{M}}_s \in [\bar{\mathcal{M}}_-, \bar{\mathcal{M}}_+]$. Under the same (reasonably large SNR) assumptions leading to (2.11), the involved joint probability density can be approximated by a gaussian bivariate [34]:

$$w(C_-, C_+) \approx \frac{\exp\left[-\dfrac{(C_- - d_-)^2 + (C_+ - d_+)^2 - 2R(C_- - d_-)(C_+ - d_+)}{2(1 - R^2)}\right]}{2\pi(1 - R^2)^{1/2}}, \tag{2.12}$$

where:

$$d_\pm = d[\Delta_\pm, \Theta_{max}(\Delta_\pm)], \quad R \approx \bar{d}[\delta_L, \Theta_{max}(\Delta_+) - \Theta_{max}(\Delta_-)], \tag{2.13}$$

and the function $\Theta_{max}(\cdot)$ has been defined in Sect. II.F and shown in Fig. 3.

Letting:

$$\bar{\mathcal{M}}_s^{-5/3} = \bar{\mathcal{M}}_q^{-5/3} + \eta\delta_L, \quad \eta \in [0,1[, \tag{2.14}$$

the false dismissal probability (2.11) is obviously a function of η. Within the limits of validity of (2.8) to (2.13), for a fixed SNR and a prescribed α, the following qualitative dependence of β on the lattice spacing δ_L is observed. In a neighbourhood of $\eta = 0.5$, the false dismissal probability is reduced by reducing the spacing δ_L among the templates. On the other hand, in a neighbourhood of $\eta = 0$, reducing the template spacing produces an *increase* of β. This is due to the dominant effect of the parallel increase of γ, needed to keep α unchanged.

A judicious tradeoff should be obviously sought, to choice a value of Γ, and hence of δ_L, via (2.6), which minimizes, e.g., the average value of β w.r.t η, under the assumption of a uniform distribution of the source chirp mass.

III. A NEARLY MINIMUM REDUNDANT INTERPOLATED LATTICE

This section contains the main new results. A short introduction to the theory of q-BL functions is included to make the paper self-contained.

A. q-BL Functions and Cardinal Expansions

A function $f : x \in [a,b] \to \mathcal{R}$ is q-BL in the L^∞ norm iff [35]:

$$\exists\ \gamma, B_c \in \mathcal{R}^+ \ : \ \sup_{x\in[a,b]} |f(x) - f_B(x)| = \exp[-\gamma(B - B_c)], \tag{3.1}$$

$f_B(x)$ being obtained by taking the inverse Fourier transform of the spectrum of $f(x)$ *chopped* at $|y| \geq B$, viz.:

$$f_B(x) = \mathcal{F}^{-1}_{y\to x}\left\{W\left(\frac{y}{B}\right) \cdot \mathcal{F}_{x\to y}\left[f(x)\right]\right\}, \tag{3.2}$$

where:

$$W(x) = \begin{cases} 1, & |x| \leq 1 \\ 0, & |x| > 1. \end{cases} \tag{3.3}$$

For a strictly bandlimited function $f(x)$, whose spectrum vanishes *identically* outside $[-B, B]$, eq. (3.2) provides an *exact* interpolating representation known as cardinal expansion [36], [37]:

$$f_B(x) = \sum_{n=-\infty}^{\infty} f(x_n)\ \mathrm{sinc}\left[\frac{\pi}{\delta}(x - x_n)\right], \quad x_{n+1} - x_n = \delta, \quad \delta = \frac{1}{2B}, \tag{3.4}$$

where $\mathrm{sinc}(x) = \sin(x)/x$. For a q-BL function on the other hand, one can prove that eq. (3.4), while reproducing *exactly* $f(x)$ at $x = x_k,\ k \in \mathcal{N}$, satisfies eq. (3.1), i.e. that

$$\forall\epsilon > 0,\ \exists\ B\ :\ \sup_{x\in[a,b]} |f(x) - f_B(x)| < \epsilon. \tag{3.5}$$

Equation (3.4) is an *approximate* sample-interpolating representation, where the sample density $\delta^{-1} = 2B$ depends on the prescribed L^∞ approximation error ϵ. It is important to note that the *exponential* decay of the error in (3.1) implies that reducing ϵ in (3.5) by orders of magnitude does *not* change the order of magnitude of B.

Usually one needs to compute $f(x)$ in a *finite* interval $[a,b]$ including only

$$N = \left\lceil \frac{(b-a)}{\delta} \right\rceil \tag{3.6}$$

samples [38]. However, using eq. (3.4) to compute $f(x)$ in $[a,b]$ requires, in principle, knowledge of an *infinite* number of samples *outside* the interval of interest. This limitation can be circumvented by using generalized (*economized*) cardinal expansions. These expansions have the general form [40]:

$$f(x) = \sum_{n=-\infty}^{\infty} f(x_n)\ \mathrm{sinc}\left[\frac{\pi}{\delta'}(x-x_n)\right]\ \theta(x-x_n),$$

$$x_{n+1} - x_n = \delta', \quad \delta' = (2\chi B)^{-1}, \quad \chi > 1 \tag{3.7}$$

where $\theta(x)$ is a suitable *windowing function* such that:

$$\theta(0) = 1, \quad \mathcal{F}_{x\to\xi}\left[\theta(x)\right] = 0,\ \forall\ \xi > (\chi-1)B, \quad \chi > 1. \tag{3.8}$$

The expansion (3.7) is nothing but the std. cardinal expansion of the function $f(x)\theta(u-x)$, whose bandwidth under the assumptions (3.8) is $B' = \chi B$, viz.:

$$f(x)\theta(u-x) = \sum_{n=-\infty}^{\infty} f(x_n)\theta(u-x_n)\ \mathrm{sinc}\left[\frac{\pi}{\delta'}\,(x-x_n)\right],$$

$$x_{n+1} - x_n = \delta', \quad \delta' = \frac{1}{2\chi B}, \tag{3.9}$$

evaluated at $u = x$. The Fourier spectrum of $f(x)\theta(u-x)$ is a *smoothed* version of the plain spectrum of $f(x)$; a judicious choice of $\theta(x)$ can thus make in principle, the *decay rate* of $f(x_n)\theta(u-x_n)$ as $|u-x_n| \to \infty$ as fast as desired [39].
The Knab window function [40]:

$$\theta(x) = K_P(x) := \frac{\sinh\left\{\pi P(1-\chi^{-1})\left[1-\left(\frac{x}{P\delta'}\right)^2\right]^{1/2}\right\}}{\left[1-\left(\frac{x}{P\delta'}\right)^2\right]^{1/2}\sinh[\pi P(1-\chi^{-1})]} \tag{3.10}$$

satisfies all constraints (3.8) and is *essentially* confined [41] in $|x| \le P\delta'$. This allows to truncate (3.7) at $|x-x_n| \approx P\delta'$, so that for any given x, *only* $\approx 2P$ samples symmetrically placed around x are *essentially* needed to reconstruct $f(x)$. The error resulting from truncation of (3.7) with (3.10) at $|x-x_n| = P\delta'$ has been discussed in [40]. A simple (and conservative) upper bound is given by:

$$\left|\sum_{|x-x_n|>P\delta'} f(x_n)\ \mathrm{sinc}\left[\frac{\pi}{\delta'}(x-x_n)\right]\ K_P(x-x_n)\right| <$$

$$< \frac{M}{\sinh[\pi P(1-\chi^{-1})]}, \quad M = \sup_{x\in[a,b]} f(x). \tag{3.11}$$

Usually, one enforces the condition:

$$\frac{M}{\sinh[\pi P(1-\chi^{-1})]} = \epsilon' \ll \epsilon, \tag{3.12}$$

where ϵ is the prescribed L^∞ error in (3.5). Equation (3.12) can be solved to express P as a function of χ,

$$P = \frac{\sinh^{-1}(M/\epsilon')}{\pi(1-\chi^{-1})}. \tag{3.13}$$

The total number of samples

$$N_T = \left\lceil\frac{(b-a)}{\delta'}\right\rceil + 2P = \left\lceil\chi\frac{(b-a)}{\delta} + 2P\right\rceil \tag{3.14}$$

needed to represent $f(x)$ in $[a,b]$ using (3.9) and (3.10), within a prescribed L^∞ error and under the constraint (3.12), can be accordingly minimized by letting:

$$\chi = 1 + \left[\frac{2\delta\ \sinh^{-1}(M/\epsilon')}{\pi(b-a)}\right]^{1/2}. \tag{3.15}$$

B. The Cardinal-Interpolated Newtonian Match

The match $\bar{D}(\Delta)$ is a q-BL function in the L^∞ norm. This can be seen from Fig. 4, where the *exponential* decay of the L^∞ error in $[0,\infty[$ between $\bar{D}(\Delta)$ and the cardinal expansion:

$$\bar{D}_B(\Delta) = \sum_{n=-\infty}^{\infty} \bar{D}(\Delta_n)\mathrm{sinc}\left[\frac{\pi}{\delta_C}(\Delta-\Delta_n)\right], \quad \Delta_{n+1}-\Delta_n = \delta_C, \tag{3.16}$$

is displayed as a function of δ_C^{-1} on a Log-Lin plot [43]. Switching back to the original variables, eq. (3.16) reads:

$$\bar{D}_B(\bar{\mathcal{M}}_s^{-5/3}-\bar{\mathcal{M}}_T^{-5/3}) := \sum_{n=-\infty}^{\infty} \bar{D}(\bar{\mathcal{M}}_s^{-5/3}-\bar{\mathcal{M}}_n^{-5/3}) \cdot \mathrm{sinc}\left[\frac{\pi}{\delta_C}\left(\bar{\mathcal{M}}_T^{-5/3}-\bar{\mathcal{M}}_n^{-5/3}\right)\right], \tag{3.17}$$

where [44]:

$$\bar{\mathcal{M}}_{n+1}^{-5/3} - \bar{\mathcal{M}}_n^{-5/3} = \delta_C. \tag{3.18}$$

Given $\bar{\mathcal{M}}_s$, the fitting factor obtained using (3.17) is given by:

$$FF = \max_{\bar{\mathcal{M}}_T} \bar{D}_B(\bar{\mathcal{M}}_s^{-5/3} - \bar{\mathcal{M}}_T^{-5/3}) =: \bar{D}_B(\bar{\mathcal{M}}_s^{-5/3} - \bar{\mathcal{M}}_*^{-5/3}). \tag{3.19}$$

It is convenient to let:

$$\bar{\mathcal{M}}_s^{-5/3} = \bar{\mathcal{M}}_q^{-5/3} + \eta\delta_C, \quad \eta \in [0,1[, \tag{3.20}$$

$$\bar{\mathcal{M}}_*^{-5/3} = \bar{\mathcal{M}}_q^{-5/3} + \eta_*\delta_C, \quad \eta_* \in [0,1[, \tag{3.21}$$

so as to rewrite (3.19) as:

$$FF = \bar{D}_B(\eta - \eta_*). \tag{3.22}$$

The difference $\eta - \eta_*$ turns out to depend on η as shown in Fig. 5, and hence the fitting factor (3.22) depends on η as shown in Fig. 6. The minimal-match condition (1.12) should again be enforced in the worst case(s), i.e., as seen from Fig.s 5, 6, for $\eta = 0.5$ and $\eta_* = \eta$, yielding:

$$\sum_{n=-\infty}^{\infty} \bar{D}\left[\left(n+\frac{1}{2}\right)\delta_C\right] \cdot \mathrm{sinc}\left[\left(n+\frac{1}{2}\right)\pi\right] = \Gamma. \tag{3.23}$$

This condition is notably *indipendent* on q, and fixes the sample spacing δ_C.

In practice, as discussed in the previous section, it is convenient to use an *economized* cardinal expansion, viz:

$$\bar{D}_B(\bar{\mathcal{M}}_s^{-5/3}-\bar{\mathcal{M}}_T^{-5/3}) := \sum_{n=-\infty}^{\infty} \bar{D}(\bar{\mathcal{M}}_s^{-5/3}-\bar{\mathcal{M}}_n^{-5/3})\Psi_n\left(\bar{\mathcal{M}}_T^{-5/3}-\bar{\mathcal{M}}_n^{-5/3}\right), \tag{3.24}$$

where (see eq.s (3.7) and (3.10)):

$$\bar{\mathcal{M}}_{n+1}^{-5/3} - \bar{\mathcal{M}}_n^{-5/3} = \delta'_C = \chi^{-1}\delta_C, \tag{3.25}$$

and:

$$\Psi_n(x) = \mathrm{sinc}\left(\frac{\pi x}{\delta'_C}\right) \cdot \frac{\sinh\left\{\pi P(1-\chi^{-1})\left[1-\left(\frac{x}{P\delta'_C}\right)^2\right]^{1/2}\right\}}{\left[1-\left(\frac{x}{P\delta'_C}\right)^2\right]^{1/2} \sinh[\pi P(1-\chi^{-1})]}. \tag{3.26}$$

As shown in the previous section, the function (3.26) is *essentially* contained in the interval: $|x| < P\delta'_C$, and hence the infinite sum in (3.24) is *essentially* restricted to:

$$\left\lceil \frac{\bar{\mathcal{M}}_T^{-5/3}}{\delta'_C} \right\rceil - P \leq n \leq \left\lfloor \frac{\bar{\mathcal{M}}_T^{-5/3}}{\delta'_C} \right\rfloor + P. \tag{3.27}$$

Capitalizing on eq. (3.11) we shall enforce the condition:

$$\frac{1}{\sinh[\pi P(1-\chi^{-1})]} = \frac{1-\Gamma}{10} \tag{3.28}$$

to guarantee that the minimal-match condition will not be affected within the last significant figure of Γ, when using using eq. (3.24) truncated according to (3.27) in place of eq. (3.17). Further, in view of eq.s (3.13) and (3.15), we shall take:

$$\chi = \chi_{opt} =: 1 + \left[\frac{2\delta_C \, \sinh^{-1}\left(\frac{10}{1-\Gamma}\right)}{\pi\left(\bar{\mathcal{M}}_{min}^{-5/3} - \bar{\mathcal{M}}_{max}^{-5/3}\right)} \right]^{1/2} \tag{3.29}$$

and:

$$P = P_{opt} =: \frac{\sinh^{-1}\left(\frac{10}{1-\Gamma}\right)}{\pi(1-\chi_{opt}^{-1})}, \tag{3.30}$$

so as to minimize the total number of correlators

$$N_C = \left\lceil \chi \, \frac{\bar{\mathcal{M}}_{min}^{-5/3} - \bar{\mathcal{M}}_{max}^{-5/3}}{\delta_C} + 2P \right\rceil. \tag{3.31}$$

needed to evaluate (3.24) throughout the range $[\mathcal{M}_{min}, \mathcal{M}_{max}]$ of $\mathcal{M}_T$.

C. The Cardinal-Interpolated Reduced Correlator

As a next step, we make the *ansatz* that an approximate representation of the reduced (newtonian) noncoherent correlator in terms of a (generalized) cardinal expansion also holds, viz. [46]:

$$C_B := \sum_{n=-\infty}^{\infty} C_n \Psi_n(\bar{\mathcal{M}}_T^{-5/3} - \bar{\mathcal{M}}_n^{-5/3}), \tag{3.32}$$

where:

$$C_n = \max_{T_{c_T}} \left| 2 \int_{f_{inf}}^{f_{sup}} \frac{A(f)\bar{T}_n^*(f)}{\Pi(f)} df \right|, \tag{3.33}$$

and the infinte sum is truncated according to (3.27).
In (3.33) the templates $\bar{T}_n$ are defined by eq.s (1.9), (1.10) and (1.16), where the (scaled) chirp masses take the values

$$\bar{\mathcal{M}}_k^{-5/3} = \bar{\mathcal{M}}_{max}^{-5/3} + k\delta'_C, \quad k = -P, -P+1, \ldots, N_C - 1 + P, \tag{3.34}$$

the interpolating functions $\Psi_n(x)$ are given by (3.26), and the parameters δ_C, χ and P are computed from the prescribed minimal match Γ as explained In Sect. IV.A.

IV. PLAIN VS. CARDINAL INTERPOLATED LATTICE

In this section we shall compare the (newtonian) cardinal-interpolated (reduced, noncoherent) correlator to the plain-lattice of (reduced noncoherent) correlators in terms of computational cost and statistical features (detection and estimation performance). The assumed noise PSD and spectral window are given by (1.21) and (1.22), respectively.

A. Computational Burden

The plain lattice template spacings δ_L and total number of correlators N_L needed to cover the range $(0.2M_\odot, 10M_\odot)$ for some values of the minimal match Γ are compared in Table I to the corresponding quantities δ_C and N_C of the cardinal interpolated correlator.

It is seen that at *any* value of the minimal match Γ, the cardinal-interpolated representation requires some 30% *less many* templates than the plain lattice.

On the other hand, evaluating (3.32) at any value $\mathcal{M}_T \neq \mathcal{M}_k$ is substantially cheaper than computing the corresponding (reduced, noncoherent) correlator.

Indeed, to use (3.32) one really needs to evaluate the interpolating functions $\Psi_n(x)$ only at a finite number of (equispaced) values of $\bar{\mathcal{M}}_T^{-5/3}$ between the samples $\bar{\mathcal{M}}_q^{-5/3}$. The corresponding values of the interpolating functions can be computed once for all, and stored in a look-up table. As a result, only $\sim 2P$ floating point operations are needed to compute (3.32) at each of the above values of $\bar{\mathcal{M}}_T^{-5/3}$, with a typical $P \sim 10^2$.

B. Statistical Features

The statistical properties of the cardinal-interpolated correlator have been compared to those of the plain-lattice via extensive Monte Carlo simulations. The number of different realizations used to derive the statistics was $\sim 10^4$.

Simulated data were sampled in time at twice the Nyquist rate. To limit running times, the minimal-match was set at $\Gamma = 0.9$, and the chirp-mass range was chosen in such a way that the longest observable waveform spanned 2^{15} time bins. In order to avoid circular-correlation artifacts, and to have equal statistics for all reduced correlators, all templates were zero-padded up to a total length of 2^{16} bins. Gaussian uncorrelated noise samples were generated using a feedback-shift-register routine from the IMSL package, featuring an extremely large period [47], followed by a Box-Müller transformation [48]. The noise samples were added to the whitened data in the spectral domain.

In the following we shall denote the cardinal-interpolated and plain lattice test-statistics as [49]:

$$C_{max}^{(C)} = \max_{\mathcal{M}_T} \sum_k C_k \Psi_k \left(\bar{\mathcal{M}}_T - \bar{\mathcal{M}}_k\right) \tag{4.1}$$

and:

$$C_{max}^{(L)} = \max_k C_k. \tag{4.2}$$

respectively. We shall denote the estimated mass, i.e., the value of $\bar{\mathcal{M}}_T$ which yields the maximum in (4.1) or (4.2) as $\mathcal{M}_{est}$, and let:

$$\bar{\mathcal{M}}_{est}^{-5/3} = \bar{\mathcal{M}}_q^{-5/3} + \eta_{est}\delta, \quad \eta_{est} \in [0, 1[, \tag{4.3}$$

$$\bar{\mathcal{M}}_s^{-5/3} = \bar{\mathcal{M}}_q^{-5/3} + \eta\delta, \quad \eta \in [0, 1[, \tag{4.4}$$

Whenever needed a suffix/superfix L, C will be used to identify the plain-lattice and cardinal-interpolated cases in (4.3), (4.4).

The CDFs of $C_{max}^{(C)}$ (dashed lines) and $C_{max}^{(L)}$ (full lines) in the absence of signal ($SNR = 0$), are compared in Fig. 7-a, for template spacings corresponding to $\Gamma = 0.9$. The corresponding PDFs are displayed in Fig. 7-b. The observed difference falls within the 3σ uncertainty interval related to the finite number of realizations.

The CDFs of $C_{max}^{(C)}$ (dashed lines) and $C_{max}^{(L)}$ (full lines) in the presence of a signal with $SNR = 6, 8, 10$ are shown in Fig. 8-a, for the (worst) case where $\eta = 0.5$ in (4.4). The corresponding PDFs are displayed in Fig. 8-b. Again, the observed differences fall within the 3σ uncertainty interval related to the finite number of realizations. Note that the

expected value always exceeds the design value $\Gamma \cdot SNR$, as might be expected as an effect of the supremum-taking operations in (1.15), (4.1) and (4.2).

As η in (4.4) changes between 0 and 0.5, the PDFs of $C_{max}^{(C)}$ and $C_{max}^{(L)}$ change in turn. The limiting PDFs corresponding to η=0 and η=0.5 are shown in Fig.s 9 and 10, for the special case SNR=8, for of $C_{max}^{(C)}$ and $C_{max}^{(L)}$.

It can be concluded that the detection performance of the cardinal interpolated (reduced, noncoherent) correlator is essentially equivalent to that of the computationally more expensive plain lattice of (reduced, noncoherent) correlators.

We turn now to a comparison of the pertinent *estimation* features. To this end we let:

$$\xi = \frac{\bar{\mathcal{M}}_{est}^{-5/3} - \bar{\mathcal{M}}_{s}^{-5/3}}{\delta} = \eta - \eta_{est}. \tag{4.5}$$

The PDFs of ξ for the cardinal-interpolated correlator at $SNR = 8$ and $\Gamma = 0.9$ is shown in Fig. 11 for $\eta = 0$ and $\eta = 0.5$.

The corresponding probabilities $P(\xi)$ for the plain lattice of correlators are shown in Fig. 12. Note that for the plain lattice of correlators, η_{est} can take only values which are integer multiples of δ_L.

Both the cardinal-interpolated correlator and the plain lattice of correlators provide *biased* estimates. The bias $E[\xi]$ becomes for both essentially independent of the SNR at sufficiently high SNR levels ($SNR \gtrsim 8$). For the cardinal-interpolated correlator the asymptotic large-SNR bias is shown in Fig. 13, which is a close akin of Fig. 5. For the plain lattice, it is displayed in Fig. 14. The cardinal-interpolated correlator is seen to exhibit a smaller bias.

The std. deviations of the cardinal-interpolated and plain lattice estimators are nearly the same. For instance, for $\eta = 0.5$ (worst case), at $SNR = 8$ one has $\sigma(\xi_L) = 1.12$ and $\sigma(\xi_C) = .92$; at $SNR = 10$ $\sigma(\xi_L) = 0.84$ and $\sigma(\xi_C) = 0.63$.

C. Extension to PN Models

The cardinal-interpolated approach can be extended in principle, to higher order PN models, provided the *structure* and q-BL properties of the (reduced) correlator are preserved. In the geometrical language of [9], this is equivalent to requiring that the chosen parameter space be (globally) flat and Euclidean [50]. This is surely the case for 1PN models [14], and almost the case for the new 0−spin 2PN coordinates proposed in [51]. One should expect an even more substantial computational saving, in view of the higher dimension of the parameter space.

V. CONCLUSIONS AND RECOMMENDATIONS

Quasi-bandlimited function approximation theory can be used to build a (nearly) minimum redundant cardinal-interpolated representations of the noncoherent correlator for detecting gravitational wave chirps. An explicit expression has been provided and tested, for the simplest case of newtonian waveforms.

The number of correlators to be computed and interpolated in order to maintain the match above a given minimal value Γ has been shown to be *substantially less* then required by the std. (lattice) approach, and the computational gain goes up with Γ. On the other hand, evaluating the cardinal-interpolated representation at any value of $\mathcal{M}_T$ is substantially cheaper than computing the corresponding correlator.

We suggest that cardinal-interpolated expansions could be used to improve the efficiency of hierarchical searches, at all hierarchical levels.

Extension to PN templates should be straighforward, in principle, insofar as the *structure* and q-BL property of the correlators is preserved, and lead to an even increased computational gain. Work in this direction is in progress.

VI. ACKNOWLEDGEMENTS

This work has been sponsored in part by the European Community through a 1998 Senior Visiting Scientist Grant to I.M. Pinto at NAO - Spacetime Astronomy Division, Tokyo, Japan, in connection with the TAMA project. I.M. Pinto wishes to thank all the TAMA staff at NAO, and in particular prof. Fujimoto Masa-Katsu and prof. Kawamura Seiji for kindly hospitality and stimulating discussions.

[1] http://www.tamago.mtk.nao.ac.jp
[2] http://www.geo600.uni-hannover.de
[3] http://www.ligo.caltech.edu
[4] http://www.virgo.infn.it
[5] D. Lorimer and E.P.J. Van der Heuvel, Mon. Not. Roy. Astron. Soc., **283**, L37, 1996.
[6] C.W. Helström, *Statistical Theory of Signal Detection*, Pergamon Press, Oxford, 1968.
[7] B.S. Sathyaprakash and S.V. Dhurandhar, Phys. Rev. **D44**, 3819, 1991.
[8] S.V. Dhurandhar and B.S. Sathyaprakash, Phys. Rev. **D49**, 1707, 1994.
[9] B. Owen, Phys. Rev. **D53**, 6749, 1996.
[10] Th. Apostolatos, Phys. Rev. **D52**, 605, 1995.
[11] Th. Apostolatos, Phys. Rev. **D54**, 2421, 1996.
[12] S.D. Mohanty, and S.V.Dhurandhar, Phys. Rev. **D54**, 7108, 1998.
[13] S.D. Mohanty, Phys. Rev. **D57**, 630, 1998.
[14] B. Owen and B.S. Sathyaprakash, Phys. Rev. **D60**, 022002, 1999.
[15] R.P. Croce, Th. Demma, V. Pierro, I.M. Pinto and F. Postiglione, Proc. 2nd TAMA Workshop, Tokyo, october 1999.
[16] The best detector of known signals in gaussian stationary noise is a likelihood-ratio test, where the likelihood ratio takes the form of a matched correlator (matched filter) [6]. For GW chirps, the coalescency phase is unknown, and bears no physical information (*nuisance* parameter). In a generalized Bayesian approach, the likelihood ratio is averaged w.r.t. the nuisance parameters [6]. The phase-averaged matched filter goes over [6] into the noncoherent correlator (1.1), under the assumption of a *uniform* phase distribution. The a-priori distribution of the coalescency-phase being unknown, it can be shown that the uniform distribution is the *least favorable one*, i.e., that detection performance would be *better* for *any* other phase distribution (R.A. Roberts, IEEE Trans. **IT-11**, 76, 1985.).
[17] S. Droz et al., Phys. Rev. **D59**, 124016, 1999.
[18] The implied *large* dimensionless parameter in the referred asymptotic expansion is essentially cT_{orb}/r_g, where T_{orb} and r_g are the source orbital period and gravitational radius.
[19] We shall ignore amplitude/phase modulation terms arising from *precessing* orbits, as discussed e.g. in [10].
[20] We shall also ignore the effect of a nonzero residual orbital eccentricity, as discussed e.g. in (A. Królak, K.D. Kokkotas and G. Schäfer, Phys. Rev. **D52**, 2089, 1995; V. Pierro and I.M. Pinto, Nuovo Cimento **B111**, 1517, 1996; K. Martel and E. Poisson, Phys. Rev. **D60**, 124008, 1999).
[21] Reduced chirp models do not include PN corrections to the amplitude. These can be consistently neglected while using phase models up to $2PN$ order included (L. Blanchet, in *Gravitational Wave Data Analysis*, M. Davier and P. Hello, Ed.s, Editions Frontieres, 1998).
[22] T_c is the time where the model's instantaneous orbital period goes to zero. The inspiral-model however ceases to be valid well before.
[23] To 2PN order, these include the chirp mass $\mathcal{M}_{\mathcal{T}}$, the reduced mass μ_T (appearing at order 1PN and above) , the spin-orbit coupling parameter β_T (appearing at order 1.5PN and above), the spin-spin coupling parameter σ_T (appearing at order 2PN and above) [11].
[24] The simultaneous observation of *several* chirps is ruled out as extremely unlikely.
[25] S.O. Rice, Bell Sys. Tech. J., **23**, 282, 1944.
[26] The coalescency phase bears no physical information, and the coalescency time is just a *bona-fide* parameter. The source physics is thus entirely contained in $\vec{\xi}$.
[27] The fitting factor concept was perhaps first applied to GW detection by Dewey (D. Dewey, PhD Thesis, MIT,1986), and extensively exploited by Apostolatos [11].
[28] Let the *observable* sources be those for which

$$d = FF \cdot SNR = FF \cdot (K/R) > d_0,$$

where R is the source distance, and K depends on the source and antenna features. For a fixed K, $d > d_0 \Longleftrightarrow R < R_{max}(FF) = K \cdot FF/d_0$. The total number of potentially *observable* sources by a set of identical antennas covering the whole celestial sphere, is thus under the assumption of a *uniform* source density ρ_S,

$$N_{tot}(FF) = \frac{4\pi}{3}\rho_S R^3_{max}(FF) = \frac{4\pi}{3}\rho_S \left(\frac{K}{d_0}\right)^3 FF^3.$$

Letting $N_{tot}(FF) = (1-\zeta)N_{tot}(1)$, where ζ is the fraction of potentially observable sources *lost* as a consequence of mismatch, one accordingly gets

$$1 - \zeta = N_{tot}(FF)/N_{tot}(1) = FF^3,$$

a result independent of K and hence valid for all sources and antenna types.
[29] As a possible refinement, one could assign *different* values of Γ to different subsets of the parameter space, on the basis, e.g., of the corresponding estimated source/event abundance/occurrence.

[30] The probability density of the reduced correlators is obviously no longer ricean. In view of the positive-definiteness of the c's, it might be expected to be described by a Fisher-Tippet distribution (J. Galambos, *The Asymptotic Theory of Extreme Order Statistics*, Wiley, NY, 1978), whose parameters will be related to

$$\max_{T_{c_T}} d$$

as well as to the size of the FFT used to compute the Fourier transform.

[31] The functions d and D attain their maximum value iff the template is perfectly matched to the signal, viz. $\Delta = \Theta = 0$, yielding $d = D = SNR$ and $\bar{d} = \bar{D} = 1$.

[32] B.S. Dhurandhar and B.F. Schutz, Phys. Rev. **D50**, 2390, 1994.

[33] Indeed, one might intuitively expect that prob$[c_h < \gamma | SNR \neq 0] \approx 1$ in (2.10) for *almost all* h, with the exception of a *few* correlators for which $\vec{\xi}_T \approx \vec{\xi}$, and $T_{c_T} \approx T_c$.

[34] The joint probability density on the r.h.s. of (2.11) could be computed exactly (B. Levine, *Fondements Theoriques de la Radiotechnique Statistique*, MIR, Moscow, 1976). However, at SNR values such that $\beta \ll 1$,

$$C_\pm = \max_\Theta c(\Delta_\pm, \Theta) \approx c[\Delta_\pm, \Theta_{max}(\Delta_\pm)]$$

where $\Theta_{max}(\Delta_\pm)$ is the *non-random* value of Θ which maximizes $d(\Delta_\pm, \Theta)$ defined in Sect. 2, and the $C_\pm$ will be gaussian distributed, with correlation coefficient given approximately by (2.13).

[35] A similar definition applies in the L^2 norm. Indeed, the theory of q-BL functions was first introduced in L^2 (D. Slepian, Proc. IEEE **61**, 292, 1976), and later reformulated in L^∞ (A. Pinkus, *N-Widths in Approximation Theory*, Berlin, Springer, 1985).

[36] Cardinal expansions were introduced and investigated in (E.T. Whittaker, Proc. Roy. Soc. Edinburgh, **35**, 181, 1915; J.M. Whittaker, Proc. Math. Soc. Edinburgh, **1** , 169, 1929). In the Electrical Engineering Literature eq. (3.4) is known as the sampling theorem (A.J. Jerri, Proc. IEEE, **65**, 1565, 1977), and is credited to Nyquist (D. Nyquist, AIEE Trans., **47**, 617, 1928) Kotel'nikov (V.A. Kotel'nikov, Izd. Rev. Upr. Svyazi RKKA, Moscow, 1933) and Shannon (C.E. Shannon, Proc. IRE, **37**, 10, 1949).

[37] The cardinal expansion (3.4) is most simply obtained by regarding the inverse Fourier transform representation:

$$f(x) = \int_{-B}^{B} dy \; F(y) \exp(j2\pi xy)$$

as a $L^2_{[-B,B]}$ scalar product, and using Parseval identity, viz.:

$$\langle f, g \rangle = \sum_n \langle f, u_n \rangle \langle g, u_n \rangle^*$$

where $f(y) = F(y)$, $g(y) = \exp(-j2\pi xy)$, and $u_n(y) = (2B)^{-1/2} \exp(jn\pi y/B)$ is the Euler-Fourier basis on $[-B, B]$.

[38] In the signal-processing Litarature this is known as the number of degrees of freedom (D. Jagerman, Bell Sys. Tech. J., **49**, 1911, 1970) of f in $[a, b]$, at the resolution-level ϵ in the L^∞ norm.

[39] Obviously, smoothing should *not* affect the spectrum of f *within* its significant bandwidth. This implies a slightly *larger* bandwidth, $\chi > 1$, and hence some degree of oversampling. .

[40] J.J. Knab, IEEE Trans., **IT-25**, 717, 1979.

[41] More specifically, its L^∞ (and L^2) norms in $|x| > Q\delta'$ vanishes exponentially in $(Q - P)$. Knab's window (3.10) is a slightly sub-optimal choice for $\theta(x)$ under the constraints (3.8). It provides possibly the best available tradeoff between the competing requirements of minimal oversampling and minimal computational burden [40]. Alternative choices are discussed in [42].

[42] M.Pawlak and U. Stadtmüller, IEEE Trans. **IT-42**, 1425, 1996.

[43] It can be shown that $\bar{D}(\Delta)$ is a q-BL function in the L^2 norm as well..

[44] One should not be worried by the formal inclusion of negative values of the (scaled) template chirp mass $\bar{\mathcal{M}}_n^{-5/3}$ in (3.17). Changing the sign of $\bar{\mathcal{M}}_n^{-5/3}$ merely produces *time-reversed* chirps.

[45] Note that in general the needed negative and positive arguments of $\bar{D}(\cdot)$ in (3.24) do *not* differ by a mere change of sign. Accordingly, the even parity of $\bar{D}(\cdot)$ does not help to reduce the number of correlators.

[46] The extension of (generalized) cardinal expansions to stochastic processes is due to Kotel'nikov, and is discussed e.g., in [42]. Note in this connection that the additive noise affecting the data does not depend on $\mathcal{M}$.

[47] K. Kankaala, J. Saarinen and T. Ala-Nissila, Comp. Phys. Comm., **86**, 209, 1995.

[48] W.H. Press, S.A. Teukolsky, W.T. Vetterling and B.P. Flannery, *Numerical Recipes in C*, Cambridge Un. Press, 1995.

[49] The maximum in (4.2) is actually taken on a discrete set of values of $\bar{\mathcal{M}}_T^{-5/3}$ which contains 10 (equispaced) samples in each interval $[\bar{\mathcal{M}}_q^{-5/3}, \bar{\mathcal{M}}_q^{-5/3} + \delta'_C]$.

[50] Under these assumptions, a straightforward multi-dimensional cardinal expansion can be written, for which the sampling intervals δ_C^i are uniform and mutually independent.

[51] T.Tanaka and H. Tagoshi, gr-qc 00011090, 2000.

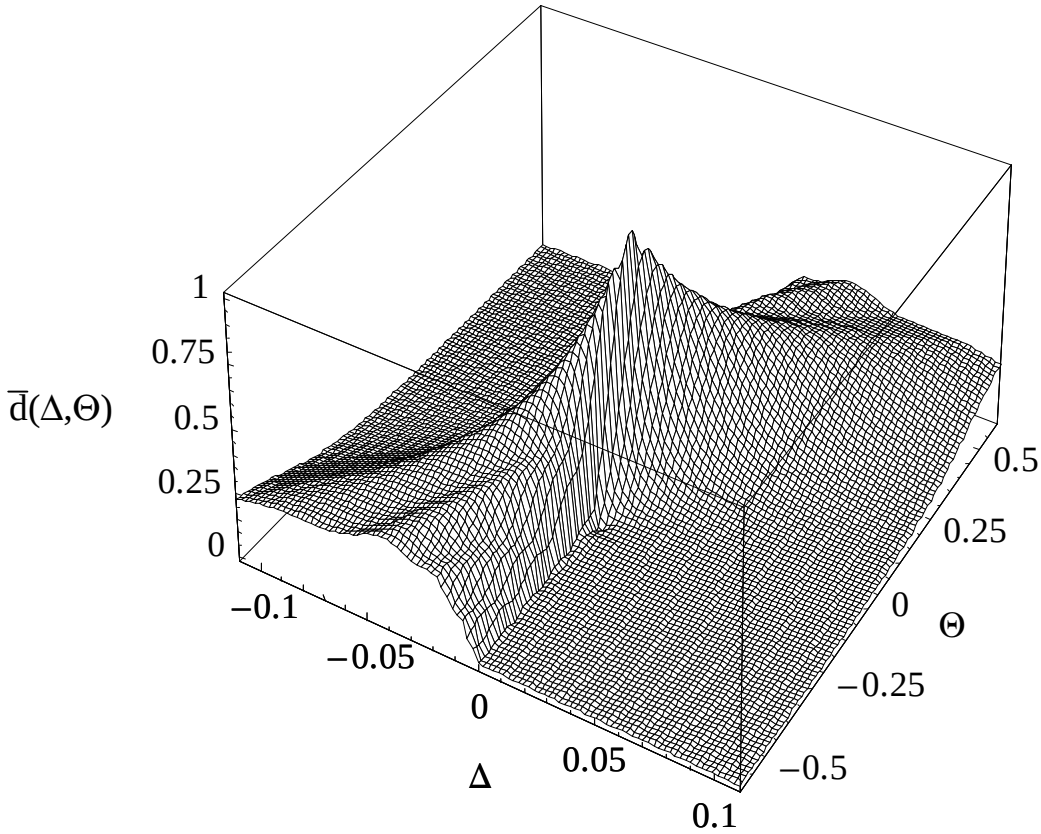

Fig. 1 – The function $\overline{d}(\Delta,\Theta)$.

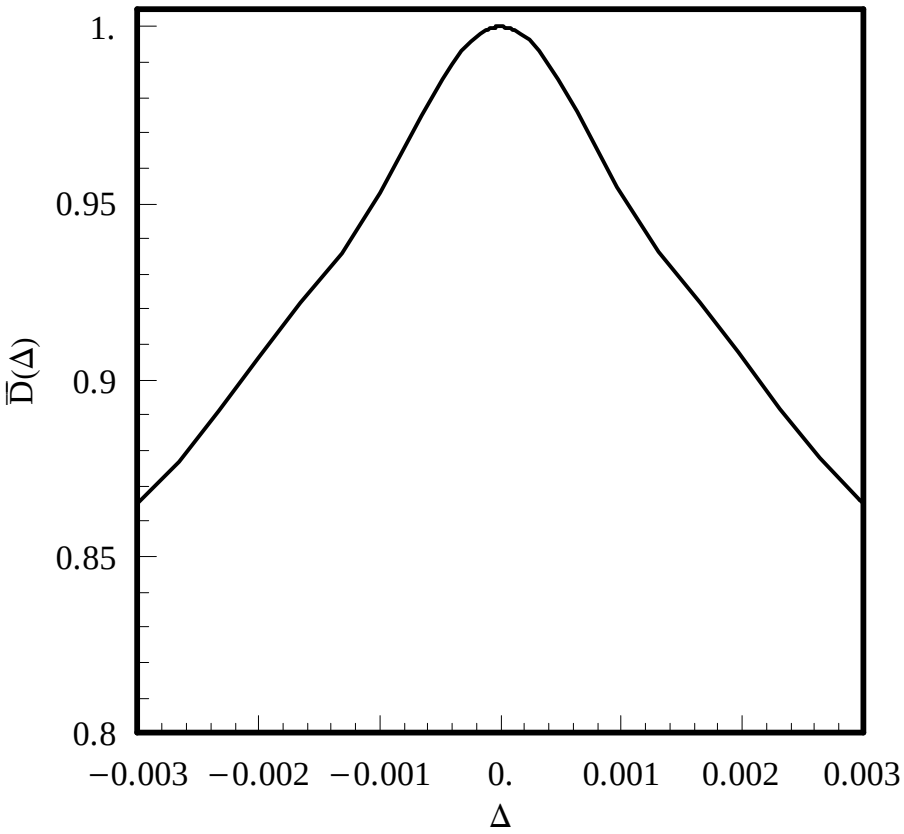

Fig. 2 – The function $\overline{D}(\Delta)$, close-up.

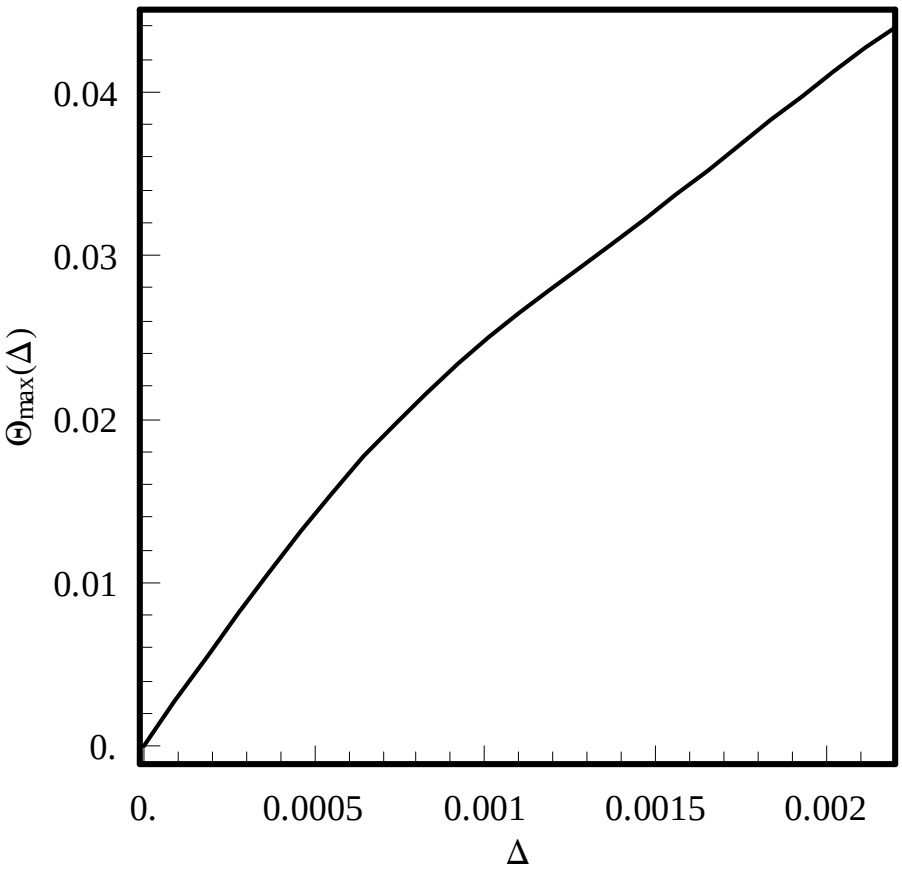

Fig. 3 – Value of Θ which maximizes $\overline{d}(\Delta,\Theta)$ as a function of Δ (close-up).

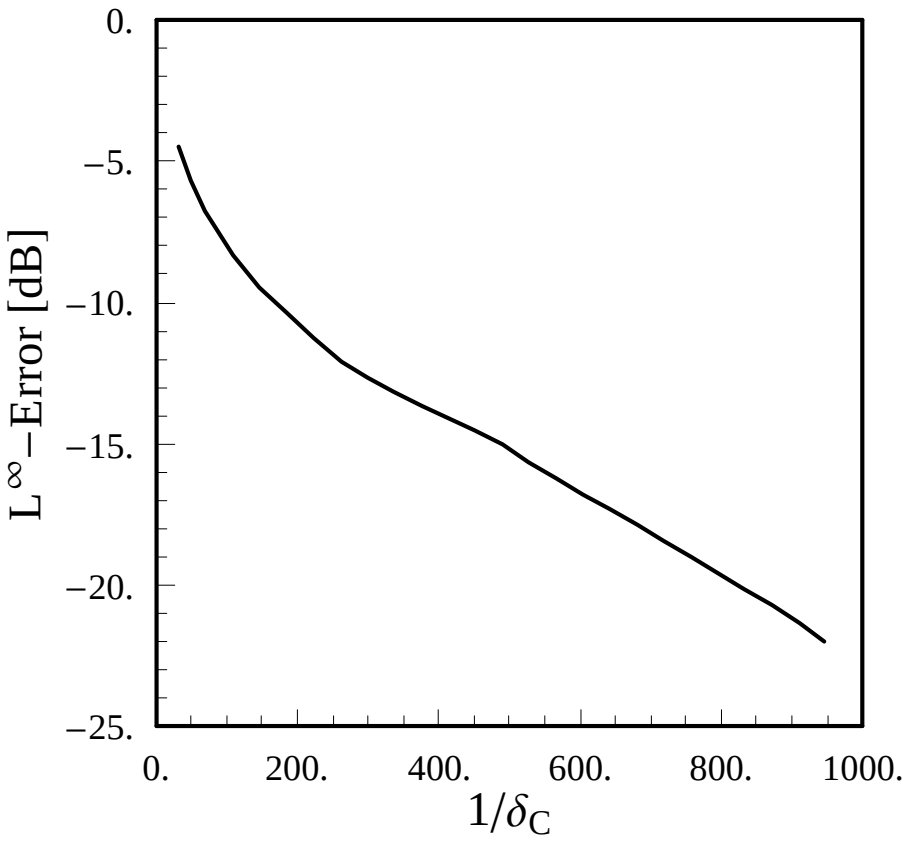

Fig. 4 - L^∞ error of cardinal expansion (52) versus sample density $1/\delta_C$.

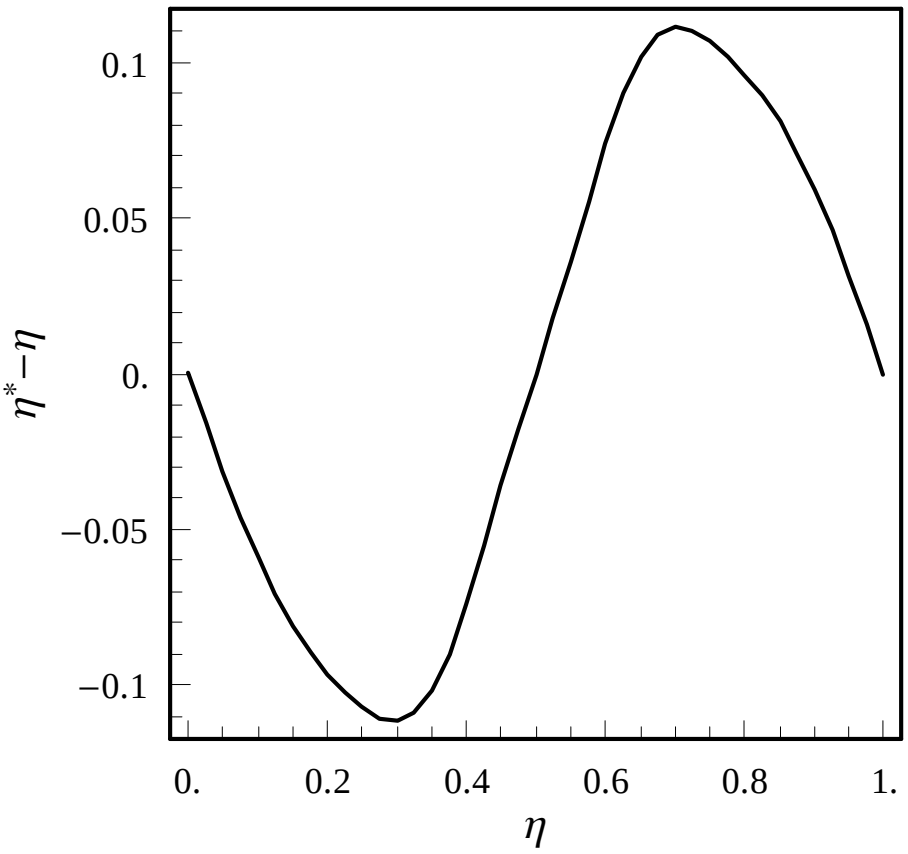

Fig. 5 – The difference η - η* as a function of η - relevant to Eq.s (52), (53).

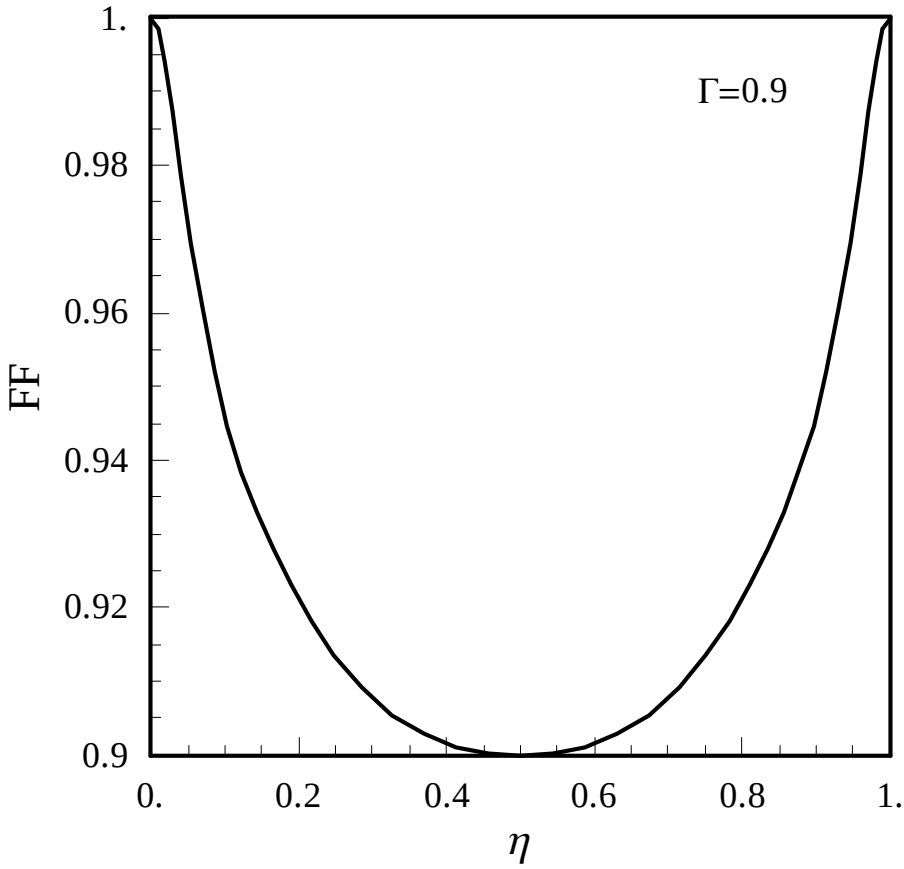

Fig. 6 – FF as a function of η, relevant to eq.s (52), (53).

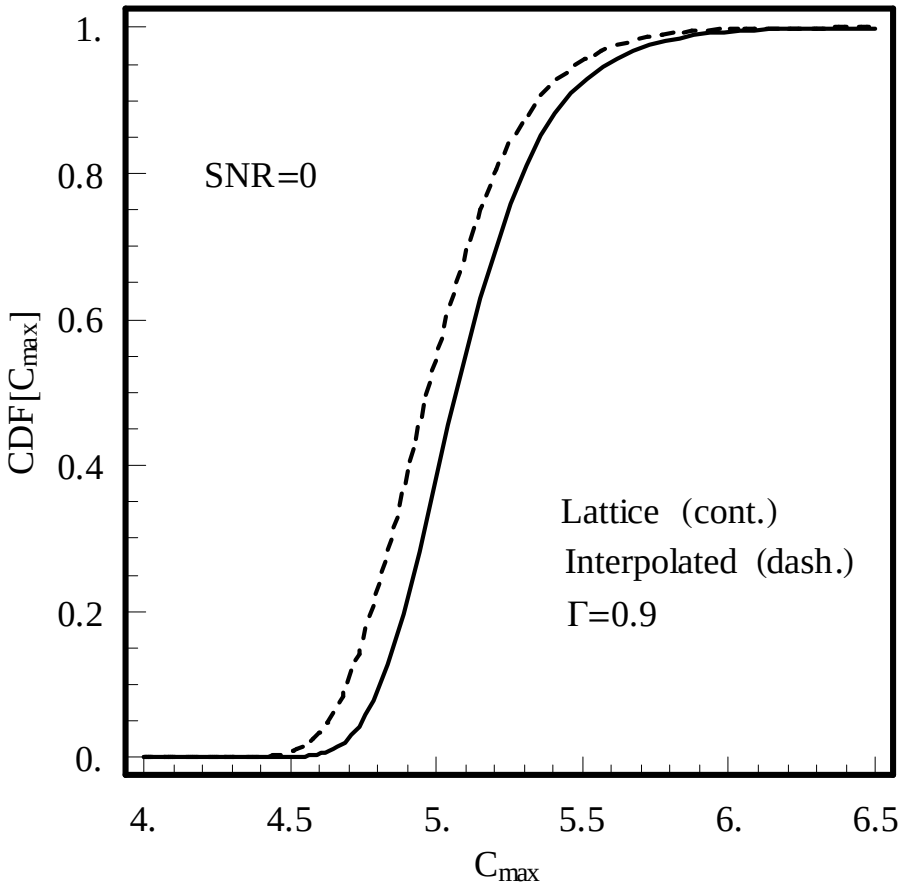

Fig. 7a –Cardinal interpolated NCC (dashed) versus plain lattice of NCCs (continuous) at Γ=0.9. CDFs of detection statistic at SNR=0.

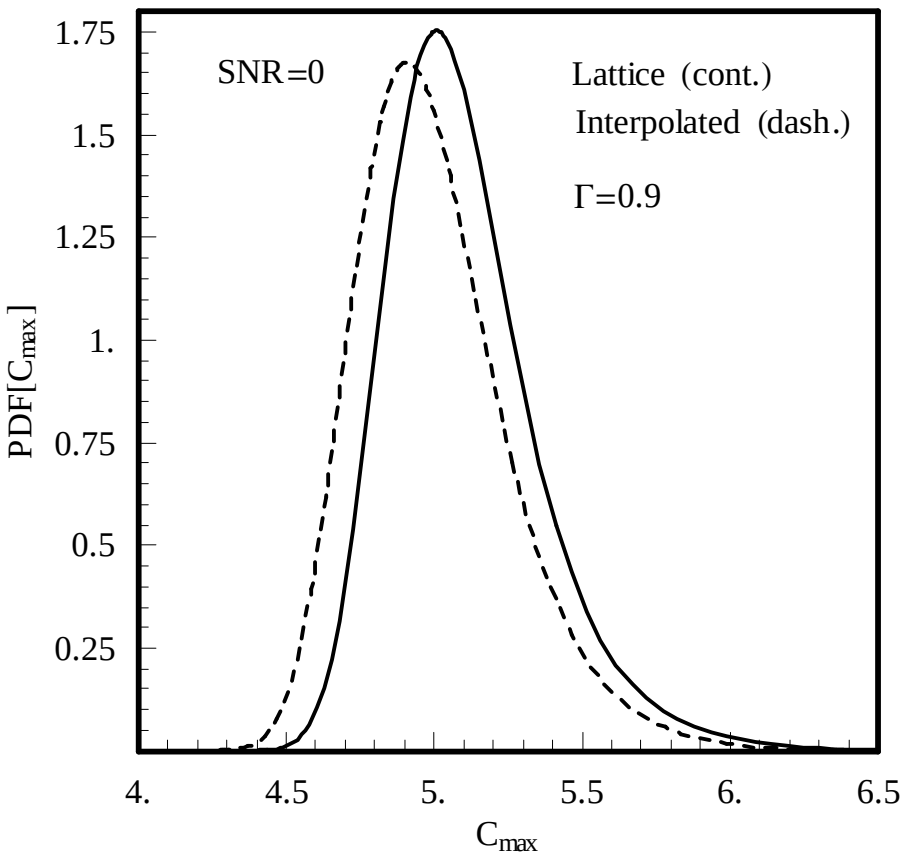

Fig. 7b –Cardinal interpolated NCC (dashed) versus raw lattice of NCCs (continuous) at Γ=0.9. PDFs of detection statistic at SNR=0.

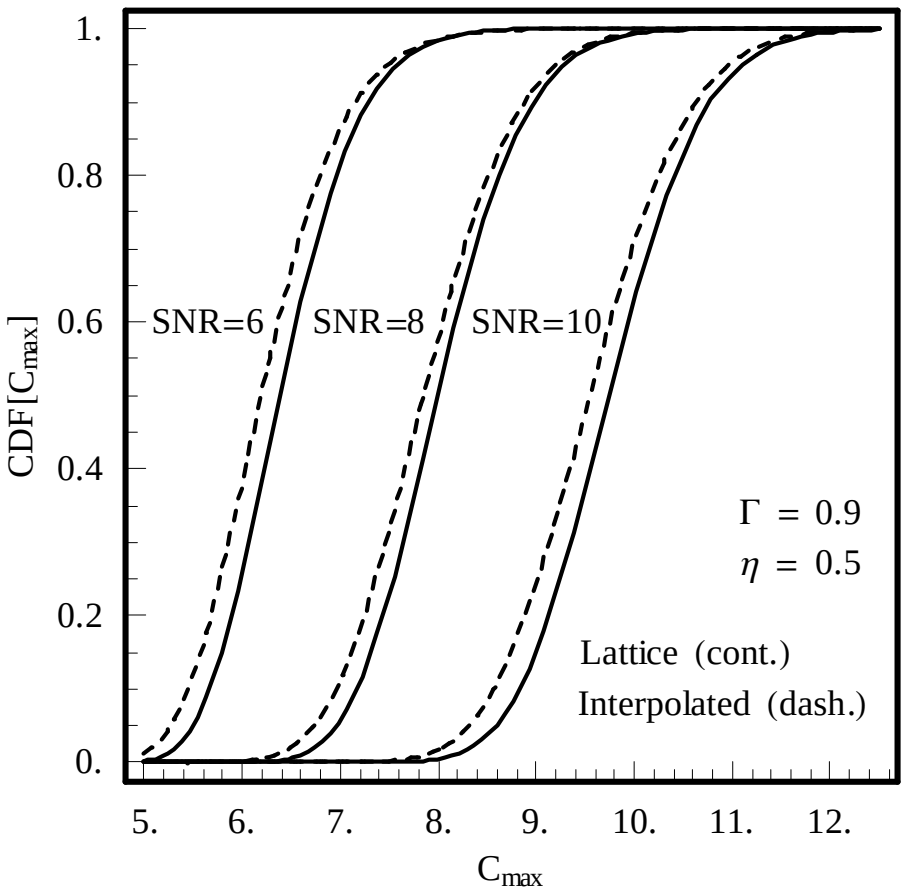

Fig. 8a –Cardinal interpolated NCC (dashed) versus raw lattice of NCCs (continuous) at Γ=0.9, η=0.5. CDFs of detection statistic at SNR=6,8,10.

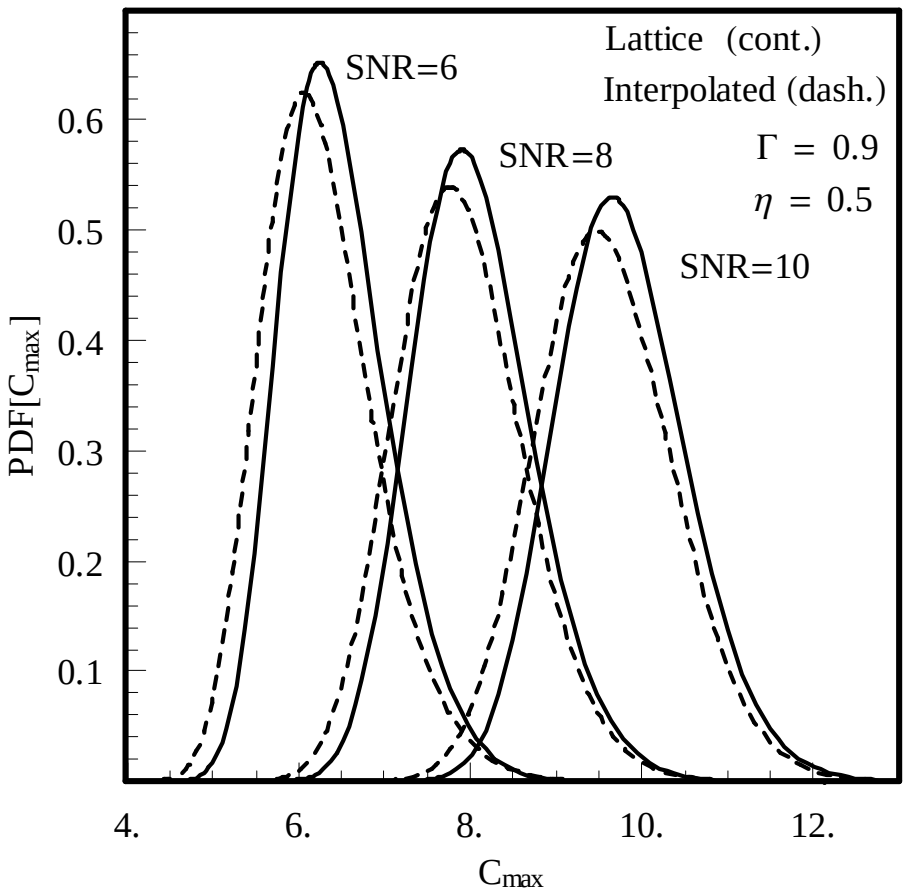

Fig. 8b –Cardinal interpolated NCC (dashed) versus raw lattice of NCCs (continuous) at Γ=0.9, η=0.5. PDFs of detection statistic at SNR=6,8,10.

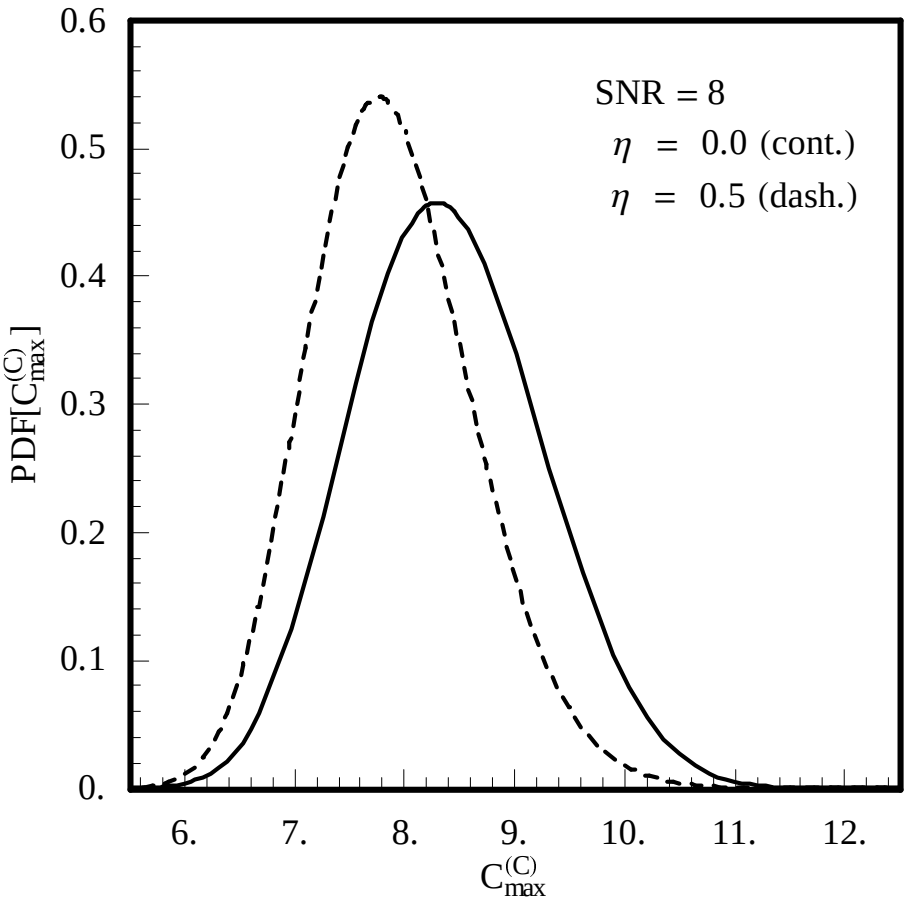

Fig. 9 – Limiting PDFs of $C^{(C)}_{max}$ at SNR=8.

Γ	δ_C	δ_L	N_C	N_L	χ_{opt}	P_{opt}
0.9	0.00596	0.00427	2635	3419	1.037	48
0.925	0.00447	0.00315	3485	4635	1.033	56
0.95	0.00307	0.00209	5029	6985	1.028	70
0.975	0.00181	0.00129	8441	11317	1.023	95
0.99	0.00121	0.00078	12553	18765	1.020	124

Table I - Plain versus cardinal interpolated lattice.

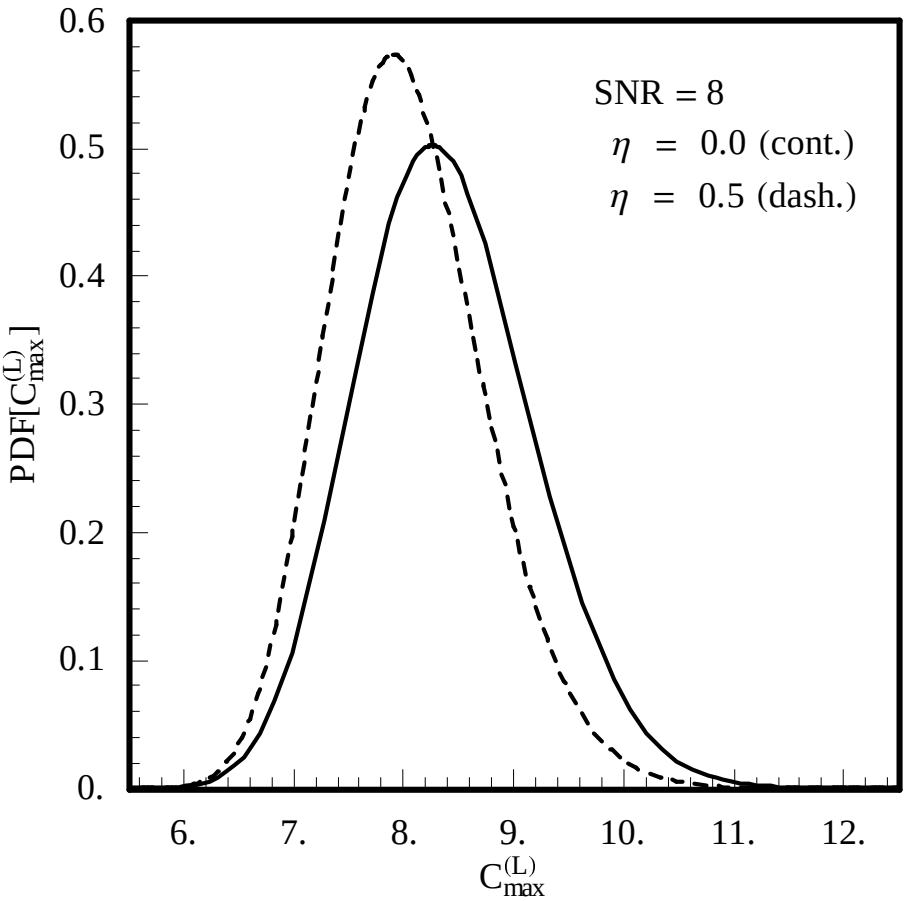

Fig. 10 – Limiting PDFs of $C^{(L)}_{max}$ at SNR=8.

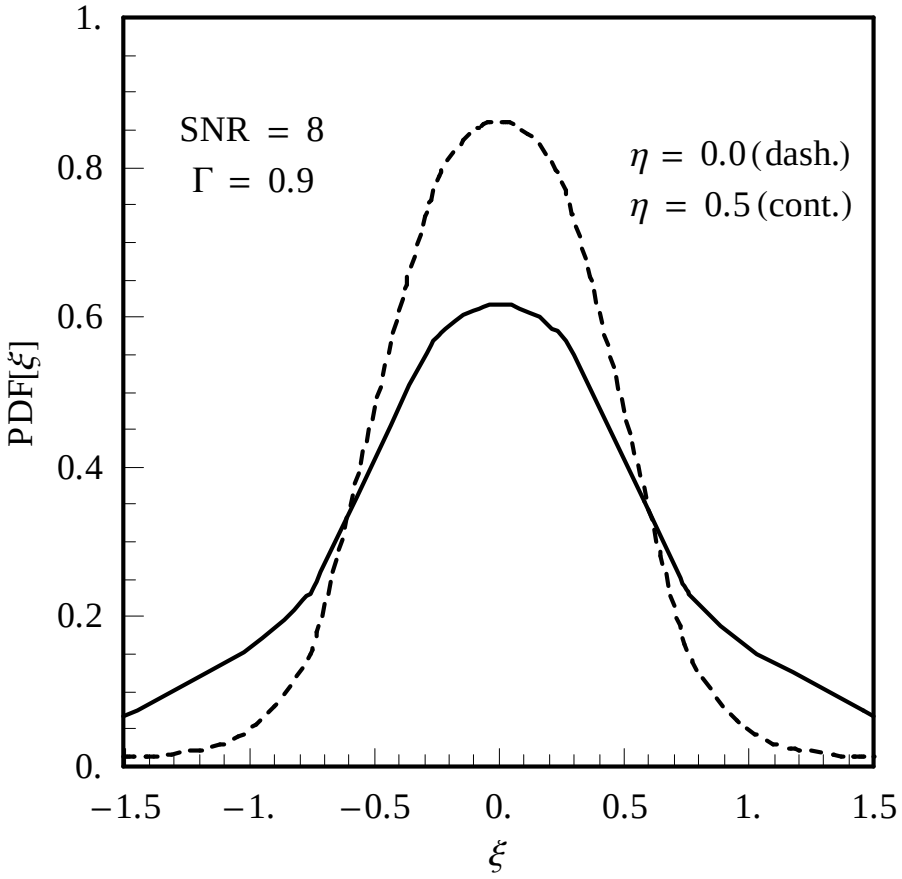

Fig. 11 – Cardinal-interpolated NCC at Γ=0.9. PDFs of estimated ξ for η=0 (dashed) and η=0.5 (continuous), at SNR=8.

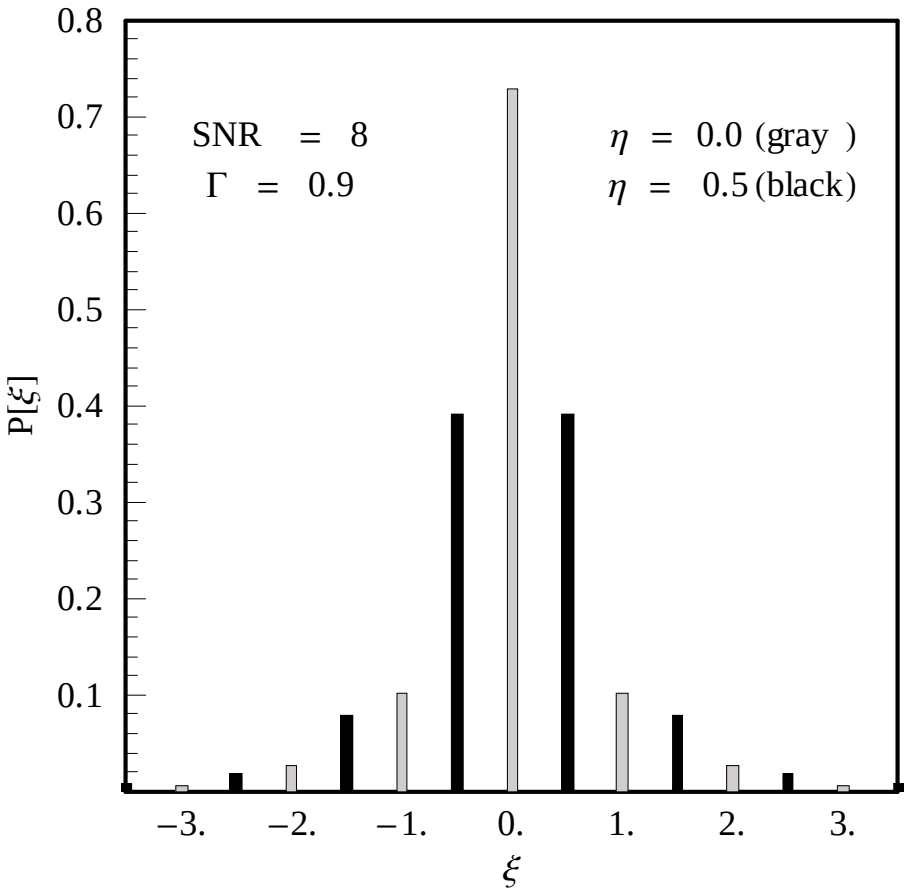

Fig. 12 – Plain lattice of NCCs at Γ=0.9. Probabilities of estimated ξ for η=0 (gray) and η=0.5 (black), at SNR=8.

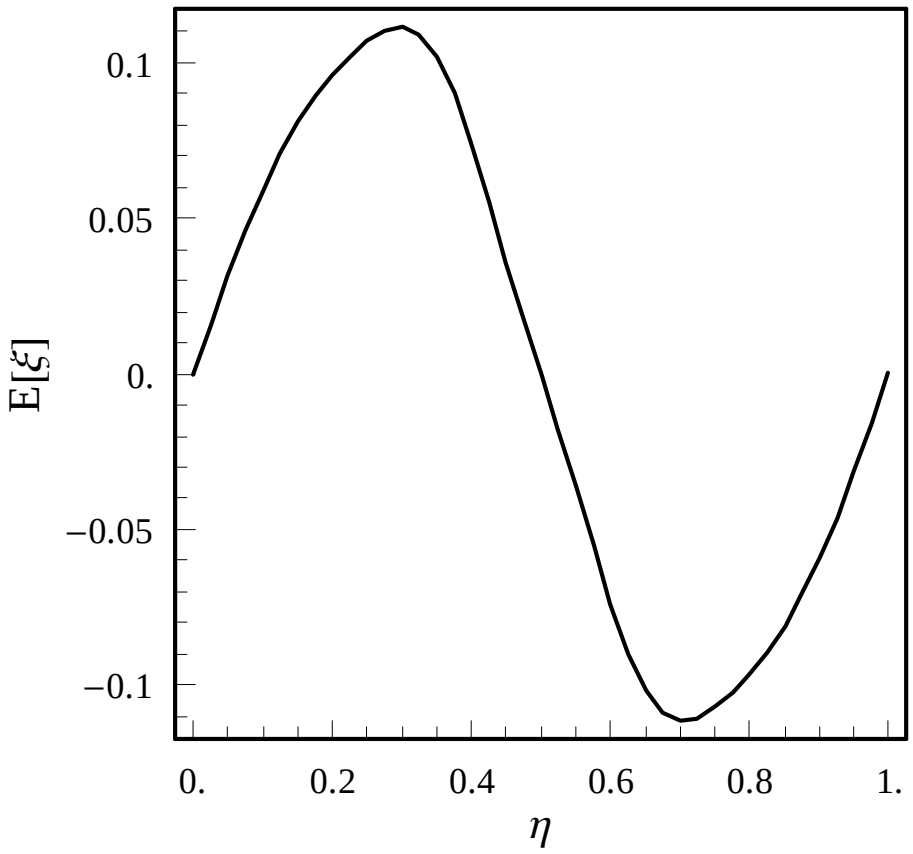

Fig. 13 – Cardinal interpolated NCC. Estimation bias (SNR ≥ 8).

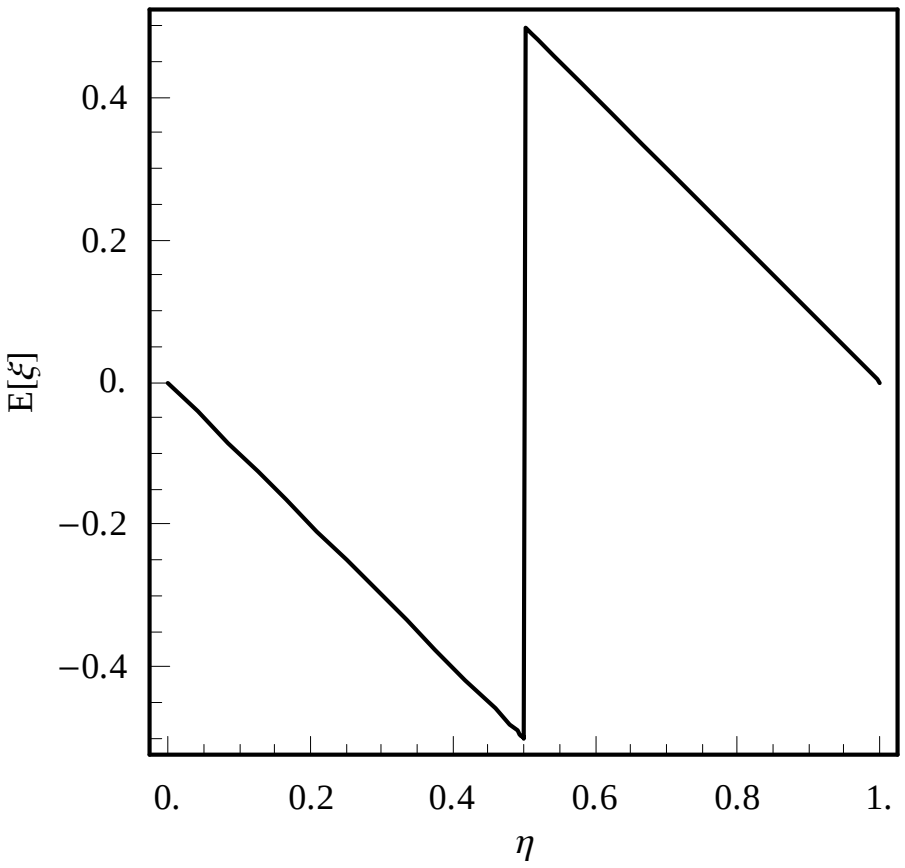

Fig. 14 – Plain lattice of NCCs. Estimation bias (SNR ≥ 8).